

Plasma resistivity profile measurement from an external radio-frequency magnetic coil

John T. Slough,^{a)} Samuel P. Andreason, and Richard D. Milroy
University of Washington Seattle, Washington 98105

(Presented on 20 April 2004; published 7 October 2004)

Plasma resistivity is obtained by measuring the change in circuit behavior from a simple loop placed externally to the plasma. The loop is part of a series-driven oscillator that can be tuned over a wide range of frequencies with a very low internal impedance. By varying the frequency, and observing both the detuning and loading of this circuit, the location and resistance of the screening currents can be determined. A two-dimensional resistive magnetohydrodynamic code calculation is performed to obtain both the plasma interaction with the oscillating field as well as the effects of nearby conductors. The plasma resistance in the numerical calculations is adjusted to match the data from the experiment and, in this way, obtain a measure of the plasma resistivity profile. © 2004 American Institute of Physics. [DOI: 10.1063/1.1783602]

I. INTRODUCTION

In this article, a simple method is described in which a key plasma parameter, the plasma resistivity, η , can be measured external to the plasma, and without a significant perturbation to the plasma. It is based on the premise that the basic response of a fully ionized plasma to an external magnetic perturbation will be fundamentally the same as that found in a simple conductor. While this is most likely not a good assumption for all magnetic perturbations, and at all frequencies (e.g., at a plasma resonance or at very low sub-Alfvénic frequencies), there is a large range of frequencies, where this assumption should be a reasonable one.¹ Whenever a time-varying magnetic field is produced near an electrical conductor, the resulting electric fields produce currents in the conductor. The magnetic field which results from the induced currents is in a direction so as to oppose the change in the applied field, and thus tends to cancel the change in the applied field within the conductor. This screening effect limits the perturbative effect on the plasma as well as localizes the induced currents.

The effect of the field change inside the conductor is thus principally manifested only by the induced currents which are dissipated as joule heat by the electrical resistance of the plasma. The resistive dissipation in this image current shows up as a power loss from the circuit that is used to produce the oscillating magnetic field. In this way, the plasma resistivity can be calculated from the measured value of the power input into the plasma from the external driven magnetic coil or loop. In effect, the plasma looks like the secondary of a transformer, and the power dissipated can be seen from the primary (see Fig. 1) as a resistance. The resistance from the “load” of the secondary circuit can be expressed as $R \propto \eta / \delta \times (f_{\text{geom}})$, where δ is the skin depth. The skin depth characterizes the depth of penetration of a high-frequency electromagnetic field where $E = E_0 e^{-r/\delta}$. The skin

depth, δ , is related to the resistivity of the plasma and frequency of the magnetic (electric) perturbation by $\delta = (2\eta / \mu_0 \omega)^{1/2}$. The dependence of the induced currents on the geometry of the coil used to generate the magnetic field and the proximity and shape of the plasma has been lumped into the parameter f_{geom} . For the simple cylindrical geometry of Fig. 1, $f_{\text{geom}} = 2\pi r_c / l_c$, where r_c and l_c are the radius and axial extent of the loop, respectively. (The resistance R is just the resistivity times length divided by cross-sectional area) For this case, one has

$$R = \frac{\sqrt{2\mu_0 \omega \pi R_w} \sqrt{\eta}}{L} \quad (1)$$

This resistance can be measured by monitoring the voltage and current that flow in the coil in Fig. 1. The average power transferred from the coil to the plasma is $P = \int_{\text{cycle}} IV dt$. The power absorbed by a resistor in a circuit is $P = \int_{\text{cycle}} I^2 R dt$, so by equating these two powers, we get

$$R = \frac{\int_{\text{cycle}} IV dt}{\int_{\text{cycle}} I^2 dt} \quad (2)$$

This is the effective resistance in the secondary. From this measure of the plasma resistance, one can obtain the plasma resistivity from Eq. (1). By varying the frequency (and therefore skin depth) and observing the change in resistance, information about the spatial variation of the plasma resistivity can also be obtained.

II. METHODOLOGY AND EXPERIMENTAL SETUP

In order to have a simple dependence resistivity on frequency, the magnetic oscillation must be relatively small ($\delta B/B \ll 1$), and in a range where there are no plasma resonances. The target plasma for the resistivity measurement was the field reversed configuration (FRC)² produced by a rotating magnetic field (RMF).³ The interest was in measuring the plasma resistivity in the azimuthal direction near the plasma separatrix where there is typically a large radial pres-

^{a)}Electronic mail: slough@aa.washington.edu

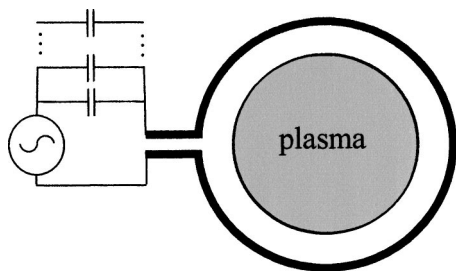


FIG. 1. Basic design of the oscillating magnetic field diagnostic. The capacitance was varied to change the series resonant frequency from 1 to 6 Mrad/s.

sure gradient.⁴ A picture of the magnetic field and coil geometry is found in Fig. 2. The diagnostic loop produced a small modulation ($\sim 2\%$) in the confining axial magnetic field near the loop with the image currents in the plasma being primarily azimuthal. Since the vacuum vessel wall was fused silica and an insulator, the loop could be placed outside the vacuum on the vacuum wall. For the experiments here, the frequency was restricted to $\omega_{LH} \gg \omega \gg \omega_{ci}$ so that there would be no possibility of coupling to ion modes or resonances in the FRC.^{5,6} The plasma response in this frequency range is the desired resistive screening of the magnetic perturbation that was applied.^{1,6}

A series-driven resonant circuit was employed as the source of the magnetic oscillation. The antenna inductance was small ($L_c \sim 1 \mu H$), so that for the range of frequencies employed, $1 < \omega < 6$ Mrad/s, the circuit impedance was only a few ohms or less. A set of 12 paralleled Insulated Gate Bipolar Transistor switches were used to drive the low impedance antenna in series with a suitably chosen capacitance to form an oscillator with a relatively high quality factor ($Q = \omega L_c / R_c \sim 30$). The advantage of this method was that it allowed for the simultaneous measure of the detuning of the resonant circuit from the change in coil inductance due to the induced plasma currents, as well as the plasma resistance from the change in Q . The plasma resistance reflected in the change of Q provided a sensitive measure of the plasma resistance with resistance changes as small as 10 m Ω could be detected. The change in resonant frequency of the oscillator is due to the large change in effective coil area over the vacuum state due to the plasma screening currents. The resonant frequency for the series circuit can be stated as

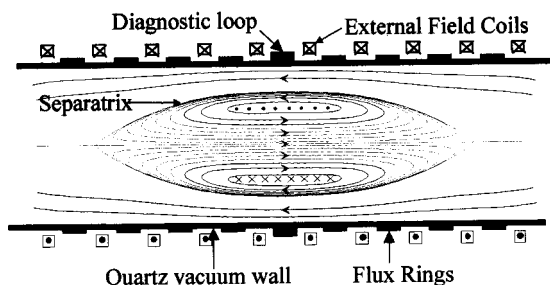


FIG. 2. Schematic showing the oscillating magnetic field diagnostic as implemented on a FRC. The loop radius was 42 cm and 6 cm in axial extent. The plasma radius ranged from 33 to 37 cm.

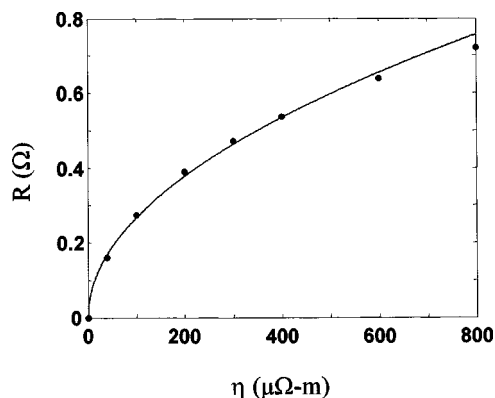


FIG. 3. Circuit resistance as a function of the plasma resistivity as determined from the 2D MHD code calculations. The resistivity profile was uniform, and the frequency was fixed at 1 MHz.

$$\omega = \frac{1}{2L} \left(\frac{L}{C} - \frac{R^2}{4} \right)^{1/2}. \quad (3)$$

The change in frequency from the vacuum ω is found by sweeping the frequency for the new resonance with the plasma present. The change in resistance can be obtained from the new Q with plasma, as well as Eq. (2). For fixed capacitance C , Eq. (3) can be used to obtain the change in inductance from the screening currents. The inductance for the simple geometry employed here (see Fig. 1) is primarily a function of the radius of the screening currents only but, for even this simple geometry, a more sophisticated model must be used to obtain quantitative information about the position of the screening currents from the changes in L . This is true for the resistance measurements as well.

A scaled physical model of the experimental arrangement in Fig. 2 was made where the plasma was replaced by cylinders of various radii and material composition. The changes in circuit resistance for resistivities from copper to stainless steel could be distinguished with this technique ($\eta < 1 \mu\Omega\text{-m}$). Radius changes on the order of 5% of the loop radius could be discerned from the observed changes in inductance. The simple relation of Eq. (1) however did not give an adequate quantitative measure of the resistivity. This was primarily due to screening currents being carried in nearby conductors as well as finite length effects.

The physical model could be used to provide the proper scaling coefficients, but a better method was to use a two-dimensional (2D) resistive magnetohydrodynamic (MHD) code⁷ to accurately account for the position of the screening currents and plasma resistance to the oscillating coil. This was particularly important for higher resistivities and larger skin depths than can be simulated with metal conductors. With the 2D model, the plasma resistivity could be specified, as well as the other parameters of the FRC (size, shape, density, temperature, etc.). The flux plot in Fig. 2, for instance, is an example of output from the code. In this way, the best calibration of the magnetic probe was attained. A plot of the circuit resistance as a function of the plasma resistivity obtained from the code results is shown in Fig. 3. It can be seen that the resistance closely follows $\eta^{1/2}$ as in Eq. (1). The geometric effect of nearby conductors was to sub-

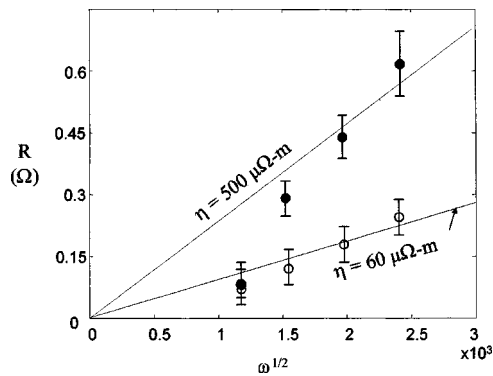


FIG. 4. Observed plasma resistive loading as a function of oscillator frequency during plasma formation (solid) and during equilibrium (open).

stantially reduce the screening currents in the plasma, which in turn reduced the magnitude of the observed circuit resistance for a given plasma resistivity. The resistance found in the numerical calculations also exhibited the $\omega^{1/2}$ dependence on frequency.

The results of experimental resistance measurements on the FRC are shown in Fig. 4. The plasma loading varied as a function of time, and the resistance measurements for two distinct times in the discharge are shown as a function of the oscillator frequency. A low resistivity is observed during the initial formation of the FRC. The edge electron temperature at this time is roughly 10 eV from Langmuir measurements, and the measured resistivity is in rough agreement with Spitzer at this time. At a later time after field reversal, when the FRC has been produced and is in a steady state, a much higher resistivity is observed. From Langmuir probe measurements, a uniform temperature of 25 eV is measured throughout this plasma. From the resistance measurements, there is clearly a very large anomalous resistivity at the plasma edge. The occurrence of this large edge resistivity is also supported by analysis of magnetic probe data together with other diagnostics.⁸ The large anomaly in resistivity at the plasma edge is most likely due to turbulence generated by the RMF in this region. The turbulent behavior is observed on other diagnostics such as the internal magnetic probes, electric field probes, and Langmuir probe. This turbulence was also observed on this diagnostic by large fluctuations in plasma loading during the discharge, which account for the larger error bars in Fig. 4. It is also apparent from Fig. 4 that as the frequency was lowered, and the skin depth increased, the plasma resistance dropped considerably more than would have been predicted by the $\omega^{1/2}$ scaling expected with a constant resistivity. The RMF is strongly attenuated as it penetrates radially inward. The lower resistivity with increasing skin depth would therefore be ex-

pected. A sharp drop in resistivity inside the separatrix is also predicted by an analysis of other probe data.⁷ The drop in resistivity was not observed in the initial lower resistivity plasma.

III. DISCUSSION

It was demonstrated that a measure of the plasma resistivity can be obtained from a loop producing an oscillating magnetic field placed external to the plasma. The particular manner in which it was implemented here was done to gain knowledge of the plasma resistance near the separatrix of the FRC. This dictated a large loop that encircled the plasma in a symmetric manner that could produce a small modulation in the axial magnetic field locally at the plasma edge. This allowed for considerable simplification in modeling the plasma response to the magnetic perturbation, as well as providing for a straightforward method for obtaining a calibration for the diagnostic. The oscillating magnetic field diagnostic however could be implemented in many different geometries, with the proper coil geometry dictated by where the plasma resistivity is to be measured. The method used here would be appropriate for any axisymmetric cylindrical discharge, such as a mirror, helicon, or plasma thruster. In most cases, some sort of multidimensional resistive MHD code calculation or physical modeling will be needed in order to assess the resistivity in a quantitative way. It is also found that it was important to take into account the effects of nearby conductors, as this had a significant effect on the calibration. The diagnostic works best with smaller plasmas with anomalous resistivities. The initial intent was to apply the magnetic loop to a plasma with a radius of 5 cm. Using values of $\omega = 1 - 5 \times 10^6$, and $\eta = 200 \mu\Omega\text{ m}$, skin depths of 0.8 to 1.8 cm are obtained. This would allow for the resistivity over a reasonable fraction of the plasma to be measured. For the much larger plasma studied here ($r \sim 35$ cm), only the edge region could be penetrated and measured, however that was the very reason for implementing the diagnostic.

¹M. A. Lieberman and A. J. Lichtenberg, *Principles of Plasma Discharges and Materials Processing* (Wiley, New York, 1994).

²J. T. Slough, A. L. Hoffman, and R. D. Milroy, *Phys. Plasmas* **2**, 2286 (1995).

³H. Y. Guo, A. L. Hoffman, R. D. Brooks, A. M. Peter, Z. A. Pietrzyk, S. J. Tobin, and G. R. Votrobeck, *Phys. Plasmas* **9**, 1985 (2002).

⁴R. E. Chrien and S. Okada, *Phys. Fluids* **30**, 3574 (1987).

⁵M. Cekic, B. A. Nelson, and F. L. Ribe, *Phys. Fluids B* **4**, 392 (1992).

⁶S. Okada, K. Yamamaka, S. Yamamoto, T. Masumoto, K. Kitano, T. Asai, F. Koderu, M. Inomoto, S. Yoshimura, M. Okubo, S. Sugimoto, S. Ohi, and S. Goto, *Nucl. Fusion* **43**, 1140 (2003).

⁷R. D. Milroy and J. U. Brackbill, *Phys. Fluids* **25**, 775 (1982).

⁸R. D. Milroy and K. E. Miller, *Phys. Plasmas* **11**, 633 (2004).